ASSESSING A GLOBAL SOURCE-RECEPTOR RELATIONSHIP OF POLYCHLORINATED BIPHENYLS USING THE FINELY-ADVANCED TRANSBOUNDARY ENVIRONMENTAL MODEL (FATE)

Kawai T[1]*, Suzuki N[1], Handoh IC[2]

[1]Research Center for Environmental Risk, National Institute for Environmental Studies (NIES), Ibaraki, Japan;
[2]The Futurability Initiatives, Research Institute for Humanity and Nature (RIHN), Kyoto, Japan

Introduction

Persistent organic pollutants (POPs) are very persistent, prone to be transported to remote regions such as the Arctic, are highly bioaccumulative and toxic, which may adversely affect human and ecosystem health. Understanding the transboundary environmental dynamics and the levels in the environment is of primary importance to evaluate the potential gains from an international approach to abatement of POPs pollution. To this end, numerical modelling is believed to be essential because of the paucity of observational data sets. During the last decades, a number of multimedia models for POPs have been developed both for regional[1], hemispheric[2] and global[3] scales. These models can successfully simulate POPs loads, sinks, and fluxes in or between environmental compartments. On the other hand, contributions of source regions to the amounts of POPs in a specific receptor region are unlikely to be estimated directly by these models. Therefore, comprehensive global-scale source-receptor (S-R) analyses are yet to be studied[4].

Recently, we developed a multimedia model for POPs, named the Finely-Advanced Transboundary Environmental model[5, 6]. In this study, we implemented a new S-R analyses option in FATE. Using this model, we estimated S-R relationships of polychlorinated biphenyls (PCBs) in the global atmosphere and the oceans.

Materials and methods

Finely-Advanced Transboundary Environmental model (FATE)

FATE is a global multimedia model that predicts biochemical cycles of POPs across and in the atmosphere, ocean, vegetation, soil, and cryosphere. FATE consists of 3D atmospheric and oceanic transport sub-models as its main dynamical cores. These sub-models enable us to predict 3D transboundary transports by the atmospheric and the oceanic general circulations with fine spatial and temporal resolutions. The spatial resolutions of the atmosphere and the ocean are 2.5°×2.5°×27 σ-layers (σ=1-0.003) and 1.0°×1.0°×50 layers (0-5500 *m* depth), respectively. Similar to the other multimedia models, FATE formulates general processes for POPs such as i) degradation and phase partitioning in model compartments, ii) dry and wet depositions, iii) diffusive near-surface inter-compartment transports, and iv) vertical transports by molecular diffusion and infiltration in the surface soil. In addition, biotransfers of POPs to primary producers such as terrestrial vegetation and marine phytoplankton are parameterized in the model using satellite-based land-cover and chlorophyll pigment concentration data, respectively.

Method for Source-Receptor Analyses

There are some different approaches that are frequently used in this research topic, including methods using marking (or tagged) tracer[7], emission sensitivity analyses[8], and/or Lagrangian dispersion/back trajectory models[9]. In this study, we adopted the emission sensitivity method, because this method is relatively widely used, and we can apply FATE to the analyses without any major modifications of the model. The method is summarized as follows:

- Perform α+1 FATE runs, where, α is the number of source regions; *i.e.*, one base run, and α perturbed runs where small perturbation of emission from a selected source region is applied.
- Compare the results from the base run and the perturbed runs to estimate changes in POPs contents in receptor regions due to the perturbed emission applied in the source regions.
- Linearly scale the changes up to the case of 100% reduction of emission to estimate the relative contributions of source regions to the POPs contents in the receptor regions.

As is evident from the procedure above, the theoretical basis of this method is to assume low-level non-linearity between changes in the POPs contents in receptor regions and the perturbed emission in source regions. Our complementary analyses suggested that this assumption appears to hold in FATE simulations (not shown).

Source and Receptor Regions

For terrestrial source regions, we defined the following 8 regions according to the classifications of the United Nations: i) Africa (AFR), ii) Latin America and the Caribbean (LAC), iii) Northern America (NAM), iv) Central, Southern, and Western Asia (CSWA), v) Eastern, South eastern Asia (ESEA), vi) Eastern Europe (EEU), vii) Northern, Southern, and Western Europe (NSWE), and viii) Oceania (OCE). These 8 regions cover whole land surfaces of the globe so that we can perform closed S-R analyses. We defined terrestrial receptor regions to the surface atmosphere (*i.e.*, atmospheric boundary layer) of the same 8 terrestrial source regions described above. For the oceans, we defined the receptor regions to the surface ocean (*i.e.*, ocean mixed layer), which is divided into the following 7 oceans based on the classifications of the International Hydrographic Organization: i) the North Pacific (NPA), ii) the South Pacific (SPA), iii) the Nouth Atlantic (NAT), iv) the South Atlantic (SAT), v) the Indian Ocean (IND), vi) the Arctic Ocean (ARC), and vii) the Antarctic Ocean (ANT). These 7 oceans also cover whole sea surfaces of the globe.

Simulation Design and Data Used

For the current work, we selected PCB153 for discussions. In total 9 runs (*i.e.*, one base run and 8 perturbed runs with 20% reduction of emission) were performed for the years 1930-2010, and the annual mean results for the year 2010 were analyzed. We have employed middle scenario of the updated Breiviks' emission inventory[10], land-cover classification from the Global Land Cover for the year 2000 (GLC2000), 6-hourly atmospheric forcing data form US National Centers for Environmental Prediction (NCEP) / National Center for Atmospheric Research (NCAR) Reanalysis 1[11], monthly oceanic forcing data from Geophysical Fluid Dynamics Laboratory (GFDL) Ocean Data Assimilation experiment[12] (ODA). The phytoplankton biomasses and growth rates are also used in FATE to parameterize bioconcentration in primary producers. These biological data are estimated from SeaWiFS-based ocean color and a Carbon-based production model[13].

Results and discussion

At first, the spatial distributions of PCB153 are discussed to clarify the regions important for discussion with relatively high PCB153 contents or average concentrations. Fig. 1 shows the annual mean (2010) of the column-integrated modelled PCB153 concentrations in (a) the atmospheric and (b) the oceanic boundary layers. As expected, both the atmospheric and oceanic concentrations in the Northern Hemisphere showed 1-2 orders of magnitude higher values than in the Southern Hemisphere (Table 1). In the atmosphere, high PCB153 concentrations are found in around Europe and the United States where historical PCB153 emissions predominated. In the oceans, high concentrations are found in the coastal seas located around Europe, and also high latitude oceans in the Northern Hemisphere such as the Arctic Ocean. In general, areas with elevated concentrations reflect several major source regions and transport pathways by both atmospheric and oceanic general circulations.

Table 1. Annual mean (2010) of the modeled PCB153 contents (C_C) and the column-integrated average concentrations (C_A) in the terrestrial and oceanic receptor regions

Terrestrial receptor regions	C_C (kg)	C_A (pg/m^2)	Oceanic receptor regions	C_C (kg)	C_A (pg/m^2)
Africa	52.9	1.8	North Pacific	6590.5	81.5
Latin America and the Caribbean	27.7	1.3	South Pacific	1902.0	21.7
Northern America	81.8	4.1	North Atlantic	10857.8	238.6
Central/Southern/Western Asia	52.1	3.4	South Atlantic	972.1	24.2
Eastern/South Eastern Asia	27.3	1.7	Indian Ocean	1164.3	16.8
Eastern Europe	69.9	3.7	Arctic Ocean	3015.6	237.9
Northern/Southern/Western Europe	77.9	17.6	Antarctic Ocean	223.2	11.1
Oceania	4.9	0.6			

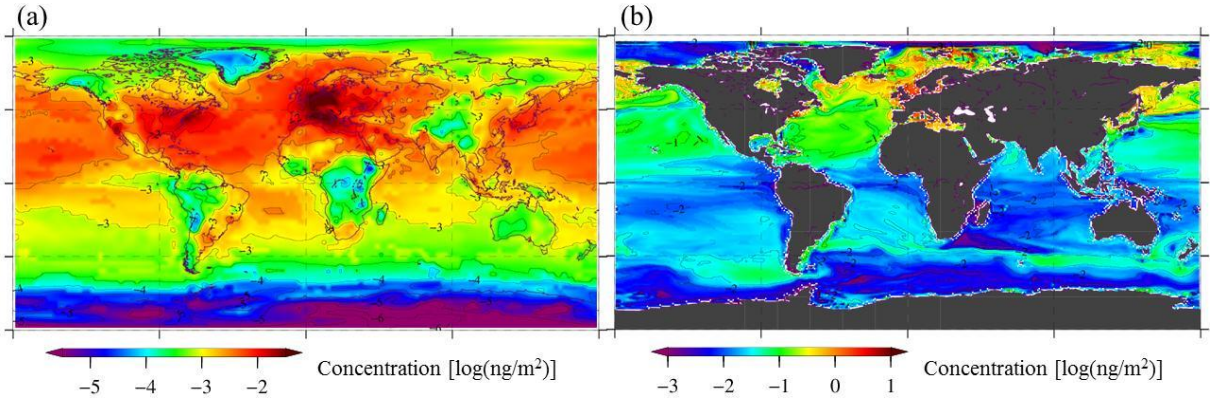

Fig. 1. Column-integrated modeled PCB153 concentrations in the planetary boundary layers. Results for (a) the atmosphere and (b) the oceans for the year 2010 are shown.

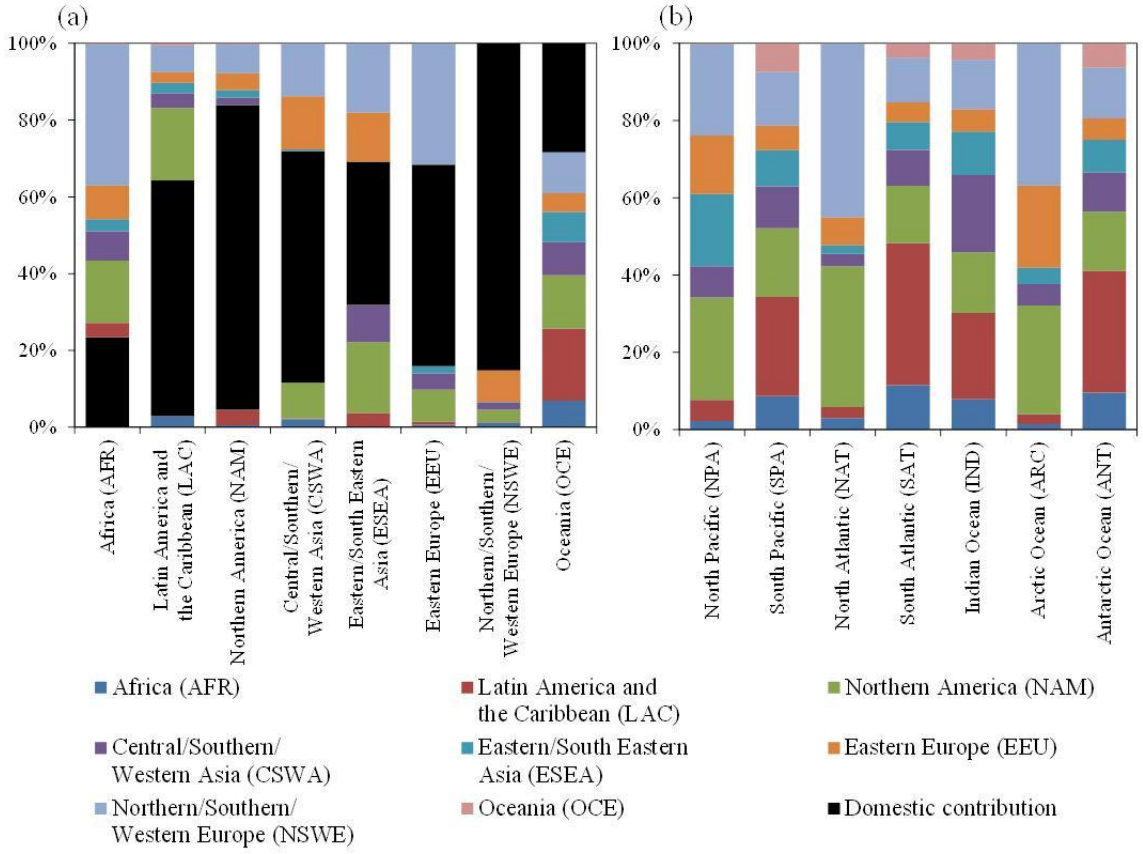

Fig. 2. Relative contributions (%) from 8 source regions to (a) 8 terrestrial and (b) 7 oceanic receptor regions for the year 2010. See the text for the definitions of the source and receptor regions.

The results of source attributions are shown in Fig. 2. In the surface atmosphere (Fig. 2a), domestic contributions (shown in black color) are dominated in all receptor regions. However, the fractions varied widely from region to region. In NAM and NSWE where relatively high C_A are found, the fractions of domestic contribution are significantly high accounted for approximately 80 % in NAM and NSWE. On the other hand, in

AFR, ESEA, and OCE, the sum of imported fractions are larger than the domestic contributions. Such differences are mainly caused by different relative contributions of emission from the source regions to the total global emission. The large imported fraction found in ESEA could also be explained by the geographical location of the region; *i.e.*, ESEA is located east the major source regions such as the Europe. Significant amount of PCB153 emitted from these major source regions could be transported by westerlies to ESEA.

In the oceans in the Northern Hemisphere, NSWE (or NSWE and EEU) and NAM are found to be major source regions. However, relative contributions of these source regions are somewhat different between receptor oceans. In ARC, Europe (NSWE and EEU) are found to be primary source region (58%). This may be explained by the proximity of the regions. In NAT, contribution from NAM (37%) are larger than that in ARC (28%), because most of the PCB153 emitted from NAM are transported eastward by temperate westerlies and the western boundary current such as the Gulf Stream. In NPA, relative contribution of ESEA (19%) is larger than those in ARC (4%) and NAT (2%). This could also be explained by the temperate westward flows in the atmosphere and the surface ocean. Contrastingly, in the oceans in the Southern Hemisphere, contributions from LAC are dominated, even though historical PCB153 emission from LAC is much smaller than that from NAM and NSWE. This implies that inter-hemispheric transports are minor transport pathway compared to the intra-hemispheric or zonal transports.

Acknowledgements
The model calculations were performed on the supercomputer system (NEC SX-8R/128M16) of the National Institute for Environmental Studies (NIES). ICH was financially supported by the Japan Society for the Promotion of Science Grants-in-Aid for Young Scientists (B) No. 24710037.

References:

1. Suzuki N, Murasawa K, Sakurai T, Nansai K, Matsuhashi K, Moriguchi Y, Tanabe K, Nakasugi O, Morita M. (2004) *Environ Sci Technol*. 38: 5682-5693.
2. Malanichev A, Mantseva E, Shatalov V, Strukov B, Vulykh N. (2004) *Environ Pollut*. 128: 279-289.
3. Guglielmo F, Lammel G, Majer-Reimer E. (2009) *Chemosphere*. 76: 1509-1517.
4. Task Force on Hemispheric Transport of Air Pollution (2010) *Hemispheric transport of air pollution 2010 Part C: Persistent Organic Pollutants*. edited by Dutchak S and Zuber A, U.N. Econ. Comm. For Europe, New York.
5. Kawai T, Handoh IC, Takahashi S. (2009) *Organohalogen Compounds*. 71: 1610-1615.
6. Kawai T, Handoh IC. (2010) *Organohalogen Compounds*. 72: 247-250.
7. Sudo K, Akimoto H. (2007) *J Geophy Res.* 112: D12302.
8. Fiore AM, Dentener FJ, Wild O, Cuvelier C, Schultz MG, Hess P, Textor C, Schulz M, Doherty RM, Horowitz LW, MacKenzie IA, Sanderson MG, Shindell DT, Stevenson DS, Szopa S, Van Dingenen R, Zeng G, Atherton C, Bergmann D, Bey I, Carmichael G, Collins WJ, Duncan BN, Faluvegi G, Folberth G, Gauss M, Gong S, Hauglustaine D, Holloway T, Isaksen ISA, Jacob DJ, Jonson JE Kaminski JW, Keating TJ, Lupu A, Marmer E, Montanaro V, Park RJ, Pitari G, Pringle KJ, Pyle JA, Schroeder S, Vivanco MG, Wind P, Wojcik G, Wu S, Zuber A. (2009) *J Geophys Res*. 114: D04301.
9. Eckhardt S, Breivik K, Li YF, Mano S, Stohl A. (2009) *Atmos Chem Phys.* 9: 6597-6610.
10. Breivik K., Sweetman A, Pacyna JM, and Jones KC. (2007) *Sci Total Environ.* 377(2): 296-307.
11. Kalnay E, Kanamitsu M, Kistler R, Collins W, Deaven D, Gandin L, Iredell M, Saha S, White G, Woollen J, Zhu Y, Chelliah M, Ebisuzaki W, Higgins W, Janowiak J, Mo KC, Ropelewski C, Wang J, Leetmaa A, Reynolds R, Jenne R, Joseph D. (1996) *Bull Ame Meteorol Soc.* 77(3): 437-472.
12. Shaoqing Z, Harrison MJ, Rosati A, Wittenberg A. (2007) *Mon Wea Rev*. 135(10): 3541-3564.
13. Behrenfeld MJ, Boss E, Siegel DA, Shea DM (2005) *Global Biogeochem Cycles.* 19(1): GB1006.